Brazilian Journal
of Chemical
Engineering

ISSN 0104-6632
Printed in Brazil
www.abeq.org.br/bjche

Vol. 29, No. 03, pp. 567 - 576, July - September, 2012

MATHEMATICAL MODELING OF A THREE-PHASE TRICKLE BED REACTOR

J. D. Silva[1*] and C. A. M. Abreu[2]

[1]Polytechnic School, UPE, Laboratory of Environmental and Energetic Technology,
Phone: + (81) 3183-7515, Rua Benfica 455, Madalena, CEP: 50750-470, Recife - PE, Brazil.
*E-mail: jornandesdias@poli.br
[2]Department of Chemical Engineering, Federal University of Pernambuco, (UFPE),
Phone + (81) 2126-8901, R. Prof. Artur de Sá 50740-521, Recife - PE Brazil.
E-mail: cesar@ufpe.br

(Submitted: August 5, 2010 ; Revised: July 27, 2011 ; Accepted: April 16, 2012)

Abstract - The transient behavior in a three-phase trickle bed reactor system (N_2/H_2O-KCl/activated carbon, 298 K, 1.01 bar) was evaluated using a dynamic tracer method. The system operated with liquid and gas phases flowing downward with constant gas flow Q_G = 2.50 x 10^{-6} m^3 s^{-1} and the liquid phase flow (Q_L) varying in the range from 4.25x10^{-6} m^3 s^{-1} to 0.50x10^{-6} m^3 s^{-1}. The evolution of the KCl concentration in the aqueous liquid phase was measured at the outlet of the reactor in response to the concentration increase at reactor inlet. A mathematical model was formulated and the solutions of the equations fitted to the measured tracer concentrations. The order of magnitude of the axial dispersion, liquid-solid mass transfer and partial wetting efficiency coefficients were estimated based on a numerical optimization procedure where the initial values of these coefficients, obtained by empirical correlations, were modified by comparing experimental and calculated tracer concentrations. The final optimized values of the coefficients were calculated by the minimization of a quadratic objective function. Three correlations were proposed to estimate the parameters values under the conditions employed. By comparing experimental and predicted tracer concentration step evolutions under different operating conditions the model was validated.
Keywords: Trickle Bed; KCl Tracer; Modeling; Transient; Validation.

INTRODUCTION

Mathematical modeling of three-phase trickle bed reactors (TBR) considers the mechanisms of forced convection, axial dispersion, interphase mass transport, intraparticle diffusion, adsorption and chemical reaction. These models are formulated by relating each phase to the others (Silva *et al*., 2003; Iliuta *et al*., 2002; Latifi *et al*., 1997; Burghardt *et al*., 1995).

The trickle-bed reactor is a three-phase catalytic reactor in which liquid and gas phases flow concurrently downward through a fixed bed of solid catalyst particles where the reactions take place. These systems have been extensively used in hydrotreating and hydrodesulfurization in petroleum refining, petrochemical hydrogenation and oxidation processes, and methods of biochemical and detoxification of industrial waste water (Al-Dahhan *et al*., 1997; Dudukovic *et al*., 1999; Liu *et al*., 2008; Ayude *et al*., 2008; Rodrigo *et al*., 2009; Augier *et al*., 2010).

The flow regimes occurring in a trickle-bed reactor depend on the liquid and gas mass flow rates, the properties of the fluids and the geometrical characteristics of the packed bed. A fundamental understanding of the hydrodynamics of trickle-bed reactors is indispensable to their design and scale-up and to predict their performance (Charpentier and Favier, 1975; Specchia and Baldi, 1977).

*To whom correspondence should be addressed

The purpose of this work was to evaluate the transient behavior of a three-phase trickle bed reactor using a dynamic tracer method to estimate the magnitude of the hydrodynamic parameters related to the operations, including the axial dispersion coefficient in the liquid phase, the liquid-solid mass transfer coefficient and the partial wetting efficiency. A dynamic phenomenological model was proposed and validated with experimental reaction data.

MATHEMATICAL MODEL

To represent the dynamic behavior of the tracer component, a one-dimensional mathematical model was formulated considering the effects related to the axial dispersion, liquid-solid mass transfer, partial wetting and chemical reaction. The model was adopted for KCl, considered to be the tracer component in the liquid phase, and was restricted to the following hypotheses: (i) isothermal operation; (ii) constant gas and liquid flow rates throughout the reactor; (iii) moderate intraparticle diffusion resistance; (iv) the chemical reaction rate within the catalytic solid is equal to the liquid-solid mass transfer rate, in any position of the reactor. The mass balance for the tracer (A_L) in the liquid phase is written as:

Mass balance for the liquid;

$$H_{d,L}\frac{\partial A_L(z,t)}{\partial t} + V_{SL}\frac{\partial A_L(z,t)}{\partial z} = D_{ax}\frac{\partial^2 A_L(z,t)}{\partial z^2} - (1-\varepsilon_s)\,F_M\;k_{LS}\,a_{LS}\left[A_L(z,t) - A_S(z,t)\right] \quad (1)$$

The initial and boundary conditions for Eq. (1) are given as:

$$A_L(z,0) = A_{L,0}\ ;\ \text{for all } z \quad (2)$$

$$\left.\frac{\partial A_L(z,t)}{\partial z}\right|_{z=0^+} = \frac{V_{SL}}{D_{ax}}\left[A_L(z,t)\big|_{z=0^+} - A_L(z,0)\right], \quad (3)$$

for $t > 0$

$$\left.\frac{\partial A_L(z,t)}{\partial z}\right|_{z=L} = 0\ ;\ \text{for } t > 0 \quad (4)$$

The equality of the mass transfer and reaction rates can be expressed by the following equations:

$$F_M\;k_{LS}\,a_{LS}\left[A_L(z,t) - A_S(z,t)\right] = \eta_S\,\varepsilon_S\,r_{KCl} \quad (5)$$

The kinetic model for the reaction was based on a first-order reaction according to the following expression (Colombo *et al*., 1976):

$$r_{KCl} = k_r\,A_s(z,t) \quad (6)$$

where r_{KCl} is the consumption rate of the reactant, $A_s(z, t)$ is the reactant concentration at the surface of the solid phase and k_r is the reaction rate constant of the first-order reaction.

Combining Equations (5) and (6), the rate of mass transfer is equal the rate of reaction at the surface of the solid phase as:

$$F_M\;k_{LS}\,a_{LS}\left[A_L(z,t) - A_S(z,t)\right] = k_r\eta_S\,\varepsilon_S\,A_S(z,t) \quad (7)$$

Equations (1) to (4) and (7) can be analyzed by employing the dimensionless variables in Table 1.

Table 1: Summary of dimensionless variables

Dimensionless concentrations	dimensionless variables
$\psi_L(\xi,t_d) = \frac{A_L(z,t)}{A_{L,0}}$	$t_d = \frac{V_{SL}\,t}{L\,H_{d,L}}$
$\psi_S(\xi,t_d) = \frac{A_S(z,t)}{A_{L,0}}$	$\xi = \frac{z}{L}$

Expressed in the dimensionless variables, the equations and the initial and boundary conditions can be rewritten as:

$$\frac{\partial\psi_L(\xi,t_d)}{\partial t_d} + \frac{\partial\psi_L(\xi,t_d)}{\partial\xi} = \frac{1}{P_E}\frac{\partial^2\psi_L(\xi,t_d)}{\partial\xi^2} - \alpha_{LS}\left[\psi_L(\xi,t_d) - \psi_S(\xi,t_d)\right] \quad (8)$$

$$\psi_L(\xi,0) = 1\ ;\ \text{for all } \xi \quad (9)$$

$$\left.\frac{\partial\psi_L(\xi,t_d)}{\partial\xi}\right|_{\xi=0^+} = P_E\left[\psi_L(\xi,t_d)\big|_{\xi=0^+} - 1\right]\ ; \quad (10)$$

for $t_d > 0$

$$\left.\frac{\partial \psi_L(\xi, t_d)}{\partial \xi}\right|_{\xi=1} = 0 \text{ for } t_d > 0 \tag{11}$$

$$\psi_L(\xi, t_d) - \psi_S(\xi, t_d) = \beta_S\ \psi_S(\xi, t_d) \tag{12}$$

Equations (8) to (12) include the following dimensionless parameters:

$$\alpha_{LS} = \frac{(1-\varepsilon_s)\, F_M\, k_{LS}\, a_{LS}\, L}{V_{SL}} \tag{13}$$

$$P_E = \frac{V_{SL}\, L}{D_{ax}} \tag{14}$$

$$\beta_S = \frac{k_r\, \eta_s\, \varepsilon_s}{k_{LS}\, a_{LS}\, F_M} \tag{15}$$

The dimensionless concentration, $\psi_S(\xi, t_d)$, was isolated in Eq. (12) and introduced into Eq. (8), reducing it to:

$$\frac{\partial \psi_L(\xi, t_d)}{\partial t_d} + \frac{\partial \psi_L(\xi, t_d)}{\partial \xi} = \frac{1}{P_E}\frac{\partial^2 \psi_L(\xi, t_d)}{\partial \xi^2} - \gamma\ \psi_L(\xi, t_d) \tag{16}$$

where,

$$\gamma = \frac{\alpha_{LS}\, \beta_S}{\beta_S + 1} \tag{17}$$

SOLUTION IN THE LAPLACE DOMAIN

Applications of the Laplace Transform (LT) to dynamic transport problems in three-phase trickle bed reactors with tracer (liquid, gas) are employed to solve the linear differential equations. To complete the solution, the Laplace Transform inversion method is indicated, where numerical inversion is often employed. In the present work, the LT technique was applied to the partial differential equation, Eq. (16), as presented below:

$$\frac{d^2\overline{\psi}_L(\xi,s)}{d\xi^2} - P_E\frac{d\overline{\psi}_L(\xi,s)}{d\xi} - P_E(s+\gamma)\,\overline{\psi}_L(\xi,s) = -\frac{P_E}{s} \tag{18}$$

where the overhead bar (–) and "s" indicate the LT and its domain variable, respectively.

The initial and boundary conditions in the Laplace domain are:

$$\overline{\psi}_L(\xi,s) = \frac{1}{s} \tag{19}$$

$$\frac{d\overline{\psi}_L(0,s)}{d\xi} = P_E\left[\overline{\psi}_L(0,s) - \frac{1}{s}\right] \tag{20}$$

$$\frac{d\overline{\psi}_L(1,s)}{d\xi} = 0 \tag{21}$$

Eq. (18) is a second-order non-homogeneous ordinary differential equation. Its solution is expressed by Eq. (22) and is composed of the general solution of the homogeneous ordinary differential equation $\overline{\psi}_{L,h}(\xi,s)$ and a particular solution $\overline{\psi}_{L,p}(\xi,s)$:

$$\overline{\psi}_{L,g}(\xi,s) = \overline{\psi}_{L,h}(\xi,s) + \overline{\psi}_{L,p}(\xi,s) \tag{22}$$

The second-order homogeneous ordinary differential equation is expressed as:

$$\frac{d^2\overline{\psi}_L(\xi,s)}{d\xi^2} - P_E\frac{d\overline{\psi}_L(\xi,s)}{d\xi} - P_E(s+\gamma)\,\overline{\psi}_L(\xi,s) = 0 \tag{23}$$

Its general solution is given by the following function:

$$\overline{\psi}_{L,h}(\xi,s) = e^{\beta_1\xi}\begin{bmatrix} C_1(s)e^{\beta_2(s)\xi} + \\ C_2(s)e^{-\beta_2(s)\xi} \end{bmatrix} \tag{24}$$

where β_1 and $\beta_2(s)$ are defined as:

$$\beta_1 = \frac{1}{2}P_E,\ \beta_2(s) = \frac{1}{2}\left[(P_E)^2 + 4P_E(s+\gamma)\right]^{1/2}$$

In term of hyperbolic functions, Eq. (24) was written as:

$$\overline{\psi}_{L,h}(\xi,s) = e^{\beta_1\xi}\begin{bmatrix} f_1(s)\sinh\beta_2(s)\xi + \\ f_2(s)\cosh\beta_2(s)\xi \end{bmatrix} \tag{25}$$

where $f_1(s)$ and $f_2(s)$ are expressed by $f_1(s) = C_1(s) - C_2(s)$, and $f_2(s) = C_1(s) + C_2(s)$.

The particular solution was given by the expression:

$$\bar{\psi}_{L,P}(\xi,s) = \frac{1}{s(s+\gamma)} \tag{26}$$

The general solution has been presented as Eq. (22), in which $\bar{\psi}_{L,h}(\xi,s)$ and $\bar{\psi}_{L,P}(\xi,s)$ were attributed according to the result below:

$$\bar{\psi}_{L,G}(\xi,s) = e^{\beta_1 \xi}\begin{bmatrix} f_1(s)\sinh\beta_2(s)\xi + \\ f_2(s)\cosh\beta_2(s)\xi \end{bmatrix} + \frac{1}{s(s+\gamma)} \tag{27}$$

where $f_1(s)$ and $f_2(s)$ are two arbitrary integration constants. Applying the boundary conditions from Eqs. (20) and (21) to the general solution, Eq. (27), led to the algebraic equations needed to find the arbitrary integration constants $f_1(s)$ and $f_2(s)$ in terms of known parameters. The expressions for these two constants have been found here as:

$$f_1(s) = -\frac{P_E\left[s\bar{\psi}_L(0,s)-1\right]}{s\left[\beta_1^2-\beta_2^2(s)\right]} \frac{\left[\beta_2(s)\sinh\beta_2(s)+\beta_1\cosh\beta_2(s)\right]}{\sinh\beta_2(s)} \tag{28}$$

$$f_2(s) = \frac{P_E\left[s\bar{\psi}_L(0,s)-1\right]}{s\left[\beta_1^2-\beta_2^2(s)\right]} \frac{\left[\beta_2(s)\cosh\beta_2(s)+\beta_1\sinh\beta_2(s)\right]}{\sinh\beta_2(s)} \tag{29}$$

Eqs. (28) and (29) were introduced into Eq. (27) to obtain the general solution of the tracer concentration in the liquid phase:

$$\bar{\psi}_{L,G}(\xi,s) = \frac{e^{\beta_1\xi}P_E\left[s\bar{\psi}_L(0,s)-1\right]}{s\left[\beta_1^2-\beta_2^2(s)\right]\sinh\beta_2(s)} \left\{\begin{matrix} -\left[\beta_2(s)\sinh\beta_2(s)+\beta_1\cosh\beta_2(s)\right]\sinh\beta_2(s)\xi + \\ \left[\beta_2(s)\cosh\beta_2(s)+\beta_1\sinh\beta_2(s)\right]\cosh\beta_2(s)\xi \end{matrix}\right\} + \frac{1}{s(s+\gamma)} \tag{30}$$

For $\xi = 1$ it was possible to obtain the concentration of the tracer at the exit of the fixed bed as follows:

$$\bar{\psi}_{L,G}(s) = \int_{\xi=0}^{\xi=1} \bar{\psi}_{L,G}(\xi,s)\delta(\xi-1)d\xi \tag{31}$$

Hence,

$$\bar{\psi}_{L,G}(s) = \frac{e^{\beta_1}P_E\left[s\bar{\phi}_L(s)-1\right]}{s\left[\beta_1^2-\beta_2^2(s)\right]} \left\{\beta_2(s)\left[\cosh\beta_2(s)\coth\beta_2(s)-\sinh\beta_2(s)\right]\right\} + \frac{1}{s(s+\gamma)} \tag{32}$$

To obtain the concentration evolution of the tracer at the exit of the trickle-bed reactor, the numerical fast Fourier transform (NFFT) technique was employed. In the NFFT operations, the Laplace variable "s" was changed to "ωi" in the Fourier domain. This technique was applied considering a step concentration disturbance at the inlet of the fixed bed, whose expression is written as:

$$\psi_{L,G}^{Cal.}(t_d) = TF^{-1}\left\{\frac{1}{(\omega i)}\bar{\psi}_{L,G}\begin{bmatrix} D_{ax}, k_{LS}, \\ F_M, (\omega i) \end{bmatrix}\right\} \tag{33}$$

MATERIAL AND METHODS

The transient behavior in a three-phase trickle bed reactor system (N_2/H_2O-KCl/activated carbon, 298 K, 1.01 bar) was evaluated by using a dynamic tracer method. The experiments were realized in a stainless steel reactor which consists of a fixed bed (0.22 m in height, 0.030 m inner diameter) of spherical catalytic pellets of activated carbon (d_p = 0.00045 m, CAQ 12/UFPE). The bed was in contact with a concurrent gas-liquid downward flow carrying the tracer in the liquid phase. Experiments were performed at constant gas flow Q_G = 2.50 x 10^{-6} m^3 s^{-1} and with the liquid phase flow (Q_L) varying in the range from 4.25x10^{-6} m^3 s^{-1} to 0.50x10^{-6} m^3 s^{-1}. Under these conditions, the low interaction regime was guaranteed (Ramachandran and Smith, 1983; Silva *et al.*, 2003). The evolution of KCl concentration was measured at the exit of the reactor as the response to a concentrations step at the reactor inlet.

Continuous analysis of the KCl tracer, fed at the reactor top at a concentration of 0.05M, was performed by using a refractive index detector (HPLC detector, Varian ProStar) at the exit of the fixed bed. The results were expressed in terms of the tracer concentration versus time.

The methodology applied to evaluate the order of magnitude of the axial dispersion, liquid-solid mass transfer coefficient and the partial wetting efficiency for the N_2/H_2O-KCl/activated carbon system was:

- Comparison of the experimental concentrations with the predicted concentrations based on the solutions of Eq. (33), developed for the system;
- Evaluation of the initial values of the parameters D_{ax}, k_{LS} and F_M from the correlations in Table 2;
- Numerical optimization of the values of the model parameters employing, as the criterion, the minimization of a quadratic objective function expressed in terms of experimental and calculated concentrations, given by Eq. (34):

$$F\left(D_{ax}, k_{LS}, F_M\right) = \sum_{k=1}^{N} \left\{ \begin{array}{c} \left[\psi_{L,G}\left(t_d\right)\right]_k^{Exp.} - \\ \left[\psi_{L,G}\left(t_d\right)\right]_k^{Cal.} \end{array} \right\}^2 \quad (34)$$

The operating conditions and the characteristics of the trickle-bed system are presented in Table 3.

Table 2: Correlations for parameter estimation. Initial values of D_{ax}, k_{LS} and F_M.

Correlations	References
$D_{ax} = 0.55\left(Re_L\right)^{0.61}$	Lange *et al*. (1999)
$\ln\left(k_{LS}\right) = 1.43 + 0.92\ln\left(V_{SL}\right)$	Tsamatsoulis and Papayannakos (1995)
$F_M = 3.40\left(Re_L\right)^{0.22}\left(Re_G\right)^{-0.08}\left(Ga_L\right)^{-0.51}$	Burghardt *et al*. (1990)

Table 3: Summary of operating conditions in the trickle-bed system (Colombo *et al*., 1976; Silva *et al*., 2003).

Category	Properties	Numerical Values
Operating Conditions	Pressure (P), bar	1.01
	Temperature (T), K	298.00
	Liquid flow $(Q_g)x10^6$, $m^3\ s^{-1}$	2.50
	Gas flow $(Q_l)x10^6$, $m^3\ s^{-1}$	4.25-0.5
	Standard acceleration of gravity $(g)x10^{-1}$, $m\ s^{-2}$	9.81
Packing and bed properties	Total bed height $(L)x10^2$, m	22.0
	Bed porosity (ε_p)	0.59
	Effective liquid-solid mass transfer area per unit column volume $(a_{LS})x10^{-2}$, $m^2\ m^{-3}$	3.97
	Diameter of the catalyst particle $(d_p)x10^4$, m	4.50
	Diameter of the reactor $(d_r)x10^2$, m	3.00
	Density of the particle $(\rho_p)x10^{-3}$, $kg\ m^{-3}$	2.56
	Reaction rate constant $(k_r)x10^3$, $kgmol\ kg^{-1}\ s^{-1}$	6.33
	Catalytic effectiveness factor (η_S)	0.89
Liquid properties	Density of the liquid phase $(\rho_l)x10^{-3}$, $kg\ m^{-3}$	1.01
	Viscosity of the liquid phase $(\mu_l)x10^{-4}$, $kg\ m^{-1}\ s^{-1}$	8.96
	Surface tension $(\sigma_l)x10^2$, $kg\ s^{-2}$	7.31
	Dynamic liquid holdup $(h_{d,l})x10^1$	4.91
	Superficial velocity of the liquid phase $(V_{SL})x10^4$, $m\ s^{-1}$	1.56
Gas properties	Density of the gaseous phase $(\rho_g)x10^1$, $kg\ m^{-3}$	6.63
	Viscosity of the gaseous phase $(\mu_g)x10^5$, $kg\ m^{-1}\ s^{-1}$	1.23
	Superficial velocity of the gaseous phase $(V_{Sg})x10^3$, $m\ s^{-1}$	16.46

RESULTS AND DISCUSSION

Experiments were performed at constant gas flow Q_G = 2.50 x 10^{-6} m^3 s^{-1} and with the liquid phase flow (Q_L) varying in the range from 0.50x10^{-6} m^3 s^{-1} to 4.25x10^{-6} m^3 s^{-1}. The experiments carried out with liquid phase flows of (0.50, 0.75, 1.25, 1.75, 2.25, 2.75, 3.25, 3.75, 4.25)x10^{-6} m^3 s^{-1} were employing to fit the model equations, while operations with liquid phase flows of (1.00, 1.50, 2.00, 2.50, 3.00, 3.50, 4.00)x10^{-6} m^3 s^{-1} were used for the model validation. Corresponding to the gas and liquid phase flows, the following superficial velocities were employed in the model equations: for the gas phase (nitrogen), V_{SG} was maintained at 10^{-3} m s^{-1}, and for the liquid aqueous solution of KCl, V_{SL} ranged from 2 x 10^{-4} m s^{-1} to 45 x 10^{-4} m s^{-1}.

The values of the axial dispersion, the liquid-solid mass transfer coefficient and the partial wetting efficiency were determined simultaneously by comparing experimental and predicted concentration data obtained at the exit of the fixed bed, subject to the minimization of the quadratic objective function (F), Eq. (34).

The numerical procedure used to optimize the values of the parameters involved the solution of Eq. (34) associated with an optimization subroutine (Silva *et al*., 2003, Box, 1965). The procedure started with initial values of the parameters until the final values were obtained, considered to be the optimized values of the three parameters when the quadratic objective function was minimized. The magnitudes of the parameters at different liquid phase flows are reported in Table 4.

Table 4: Optimized values of the parameters axial dispersion, liquid-solid mass transfer coefficient and wetting efficiency. Conditions: N_2/H_2O-KCl/ activated carbon, 298 K, 1.01 bar, Q_G = 2.50x10^{-6} m^3 s^{-1}.

Liquid Phase Flows	Optimized Values			Objective Function
Q_L x 10^6 m^3 s^{-1}	D_{ax} x 10^7 m^2 s^{-1}	k_{LS} x 10^6 m s^{-1}	F_M	F x 10^4
4.250	6.986	6.109	0.581	2.974
3.750	6.038	5.108	0.573	2.832
3.250	5.107	4.163	0.564	2.739
2.750	4.201	3.275	0.554	2.643
2.250	3.321	2.461	0.544	2.536
1.750	2.475	1.718	0.529	2.456
1.250	1.669	1.061	0.511	2.399
0.750	0.918	0.512	0.485	2.271
0.500	0.572	0.286	0.465	2.179

The axial dispersion, the liquid-solid mass transfer coefficient and the wetting efficiency are influenced by changes in the liquid flow. To represent the behavior of D_{ax}, k_{LS} and F_M, their optimized values were employed and empirical correlations formulated as Eqs. (35), (36) and (37). These are restricted to the following operational conditions:

$d_P = 3.90 \times 10^{-4}$, $1.49 \le Re_L \le 1.75$, $0.90 \le Sc_L \le 4.22$.

$$D_{ax} = 35.0901\left(Re_L\right)^{1.1701},$$
$$R^2 = 0.9987.7;\ 4.250 \times 10^{-6} m^3 s^{-1} \le Q_L \le 0.500 \times 10^{-6} m^3 s^{-1} \quad (35)$$

$$k_{LS} = 9.5602\left(Re_L\right)^{1.4303}\left(Sc_L\right)^{0.4701},$$
$$R^2 = 0.9968;\ 4.250 \times 10^{-6} m^3 s^{-1} \le Q_L \le 0.500 \times 10^{-6} m^3 s^{-1} \quad (36)$$

$$F_M = 2.7901\left(Re_L\right)^{0.1041},$$
$$R^2 = 0.9972;\ 4.250 \times 10^{-6} m^3 s^{-1} \le Q_L \le 0.500 \times 10^{-6} m^3 s^{-1} \quad (37)$$

The parameter correlations were fitted by the least-squares method. The mean relative errors (MRE) between the predicted and experimental parameter values of D_{ax}, k_{LS} and F_M in the k experiments were computed as follows:

$$MRE(p) = \frac{1}{n}\sum_{k=1}^{n}\left|\frac{(p)_k^{Pred.} - (p)_k^{Exp.}}{(p)_k^{Exp.}}\right| \times 100;$$

$p = D_{ax}, k_{LS}$ and F_M . Figures 1, 2 and 3 present parity plots of the correlated results. The mean relative errors of D_{ax}, k_{LS} and F_M at different liquid flows are shown in Table 5.

Table 5: Mean relative errors of D_{ax}, k_{LS} and F_M at different liquid flows

MRE_{Dax} (%)	MRE_{kLS} (%)	MRE_{FM} (%)
0.012	0.026	0.040
0.047	0.027	0.045
0.044	0.028	0.040
0.054	0.027	0.038
0.056	0.029	0.042
0.039	0.029	0.042
0.019	0.026	0.045
0.012	0.025	0.050
0.010	0.025	0.051

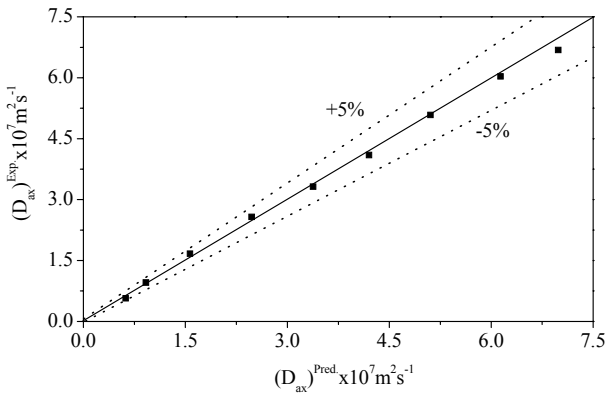

Figure 1: Parity $(D_{ax})^{Exp}$ versus $(D_{ax})^{Calc}$ for the system N_2/H_2O-KCl/activated carbon operating in the low interaction regime. Conditions: 298 K, 1.01 bar, Q_G = 2.50 x 10^{-6} m^3s^{-1}, Q_L = (4.25 to 0.50) x 10^{-6} m^3s^{-1} according to Table 4.

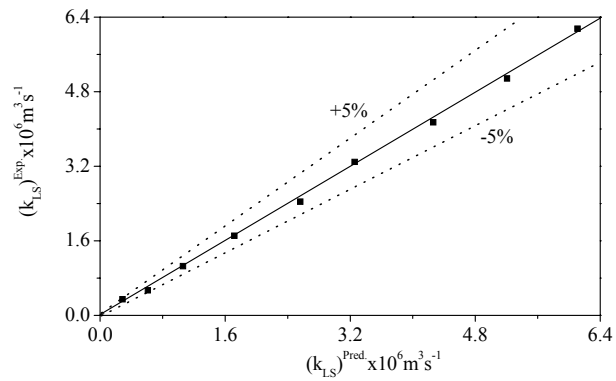

Figure 2: Parity $(k_{LS})^{Exp}$ versus $(k_{LS})^{Calc}$ for the system N_2/H_2O-KCl /activated carbon operating in the low interaction regime. Conditions: 298 K, 1.01 bar, Q_G = 2.50 x 10^{-6} m^3s^{-1}, Q_L = (4.25 to 0.50) x 10^{-6} m^3s^{-1} according to Table 4.

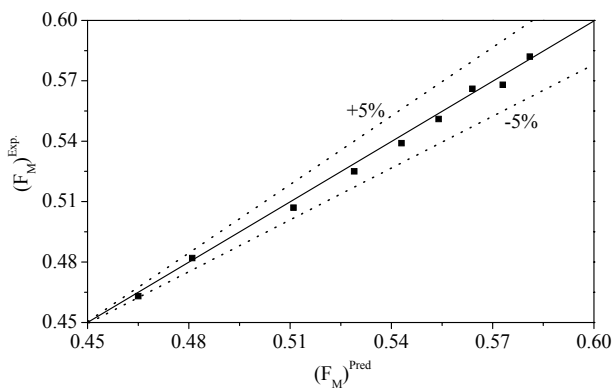

Figure 3: Parity $(F_M)^{Exp}$ versus $(F_M)^{Calc}$ for the system N_2/H_2O-KCl /activated carbon operating in the low interaction regime Conditions: 298 K, 1.01 bar, Q_G = 2.50 x 10^{-6} m^3s^{-1}, Q_L = (4.25 to 0.50) x 10^{-6} m^3s^{-1} according to Table 4.

A model validation procedure was established by comparing the predicted concentrations obtained with the values of the parameters from the proposed correlations (Eqs. (35), (36) and (37)) and experimental data not employed in the model adjustment. Table 6 presents the values of the parameters.

Figures 4 to 6 represent the model validations for three different operating conditions, where the parameter values were obtained from Eqs. (35), (36) and (37).

Table 6: Values of the axial dispersion, liquid-solid mass transfer coefficient and wetting efficiency applied to the model validation. Conditions: N_2/H_2O-KCl/activated carbon, 298 K, 1.01 bar, Q_G = 2.50 x 10^{-6} m^3 s^{-1}

Liquid Phase Flows	Parameters values calculated by the correlations (Eqs. (35), (36) and (37))		
Q_L x 10^6 m^3 s^{-1}	D_{ax} x10^7 m^2 s^{-1}	k_{LS} x 10^6 m s^{-1}	F_M (-)
4.000	6.505	5.576	0.572
3.500	5.565	4.607	0.564
3.000	4.646	3.695	0.556
2.500	3.754	2.847	0.545
2.000	2.892	2.069	0.532
1.500	2.065	1.371	0.517
1.000	1.285	0.768	0.496

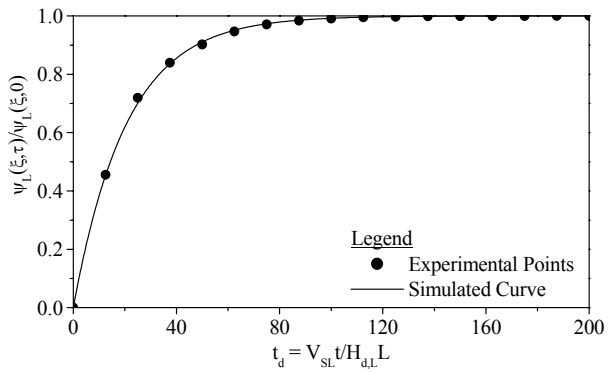

Figure 4: Evolution of the tracer concentration at the outlet of the trickle-bed reactor. Model validation. Conditions: 298 K, 1.01 bar, Q_G = 2.50 x $10^{-6}m^3$ s^{-1}, Q_L = 1.50 x $10^{-6}m^3$ s^{-1}, D_{ax} = 2.065 x 10^{-7} m^2s^{-1}, k_{LS} = 1.371 x 10^{-6} m s^{-1} and F_M = 0.517

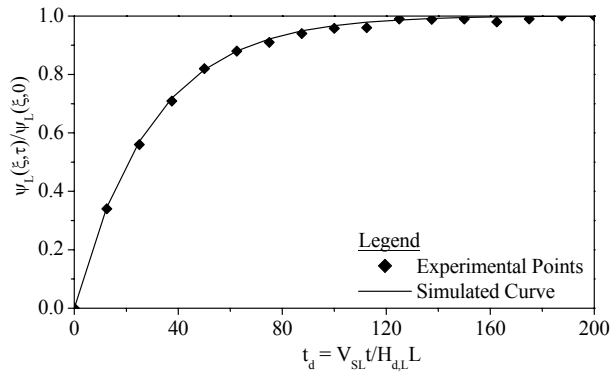

Figure 5: Evolution of the tracer concentration at the outlet of the trickle-bed reactor. Model validation. Conditions: 298 K, 1.01 bar, Q_G = 2.50 x $10^{-6}m^3$ s^{-1}, Q_L = 2.50 x $10^{-6}m^3$ s^{-1}, D_{ax} = 3.754 x 10^{-7} m^2s^{-1}, k_{LS} = 2.847 x 10^{-6} m s^{-1} and F_M = 0.545

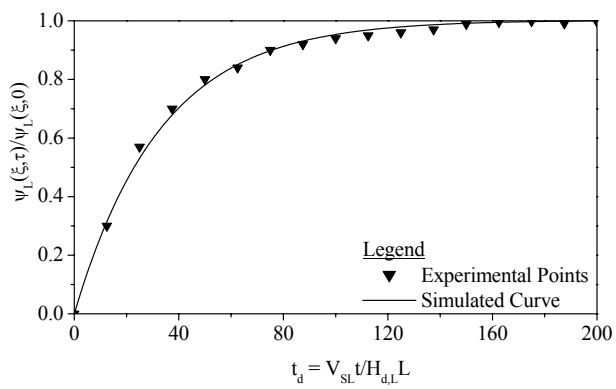

Figure 6: Evolution of the tracer concentration at the outlet of the trickle-bed reactor. Model validation. Conditions: 298 K, 1.01 bar, Q_G = 2.50 x $10^{-6}m^3$ s^{-1} and Q_L = 3.50 x $10^{-6}m^3$ s^{-1}, D_{ax} = 5.565 x 10^{-7} m^2s^{-1}, k_{LS} = 4.607 x 10^{-6} m s^{-1} and F_M = 0.564

CONCLUSIONS

The transient behavior of the three-phase trickle bed system N_2/H_2O-KCl/activated carbon was evaluated via an experimental dynamic method and via predictions of a phenomenological mathematical model. Operating at 298 K under 1.01 bar with liquid and gas phases flowing downward under constant gas flow Q_G = 2.50 x 10^{-6} m^3 s^{-1} and the liquid phase flow (Q_L) varying in the range from 4.25x10^{-6} m^3 s^{-1} to 0.50x10^{-6} m^3 s^{-1}, the concentration of KCl was measured at the exit of the reactor in response to a concentration step at the reactor inlet.

The solutions of the model equations predicted concentration profiles of the tracer employing optimized values of the parameters for the axial dispersion coefficient in the liquid phase, the liquid-solid mass transfer coefficient and the partial wetting efficiency. The magnitudes of the parameters were in the following ranges: D_{ax} = 6.986 x 10^{-7} m^2 s^{-1} to 0.572 x 10^{-7} m^2 s^{-1}, k_{LS} = 6.109 x 10^{-6} m s^{-1} to 0.286 x 10^{-6} m s^{-1} and F_M = 0.581 to 0.465. These results led to the proposal of three empirical correlations to quantify the influence of liquid phase flow rate changes on the axial dispersion, liquid-solid mass transfer and wetting efficiency in the low interaction regime.

Based on the values of the parameters indicated by the correlations, the model was validated by comparing their predictions with those obtained in different three-phase operations with mean quadratic deviations between experimental and predicted concentrations on the order of 10^{-4}.

ACKNOWLEDGMENTS

The authors would like to thank CNPq (Conselho Nacional de Desenvolvimento Científico e Tecnológico) for financial support (Process 483541/07-9).

NOMENCLATURE

$A_L(z,t)$	Concentration of the tracer in the liquid phase	kg m^{-3}
$A_S(z,t)$	Concentration of the tracer on the external surface of solid	kg m^{-3}
a_{LS}	Effective liquid-solid mass transfer area per unit column volume	m^2 m^{-3}
D_{ax}	Axial dispersion coefficient for the tracer in the liquid phase	m^2 s^{-1}
d_P	Diameter of the catalyst particle	m
d_r	Diameter of the reactor	m
F	Quadratic objective function	
F_M	wetting factor	dimensionless
Ga_L	Galileo number	$G_{a_L} = d_p^3 g \rho_L^2 / \mu_L$
$H_{d,L}$	Dynamic liquid holdup	dimensionless
i	Complex number $\sqrt{-1}$	
k_r	Reaction constant	kgmol kg^{-1} s^{-1}
L	Height of the catalyst bed	m
P_E	Peclet number	$P_E = V_{SL} L / D_{ax}$
Q_G	Gas phase flow	m^3 s^{-1}
Q_L	Liquid phase flow	m^3 s^{-1}
Re_L	Reynolds number	$Re_L = V_{SL} \rho_L d_R / \mu_L$
Sc_L	Schmidt number	$Sc_L = \mu_L / \rho_L D_{ax}$
t	Time	s
V_{SG}	Superficial velocity of the gas phase	m s^{-1}
V_{SL}	Superficial velocity of the liquid phase	m s^{-1}
z	Axial distance of the catalytic reactor	m

Greek Letters

α_{LS}	Parameter defined in Eq. (13)	dimensionless
β_S	Parameter defined in Eq. (15)	dimensionless
ε_P	internal porosity	dimensionless
$\Psi_i(\xi,t_d)$	Dimensionless concentration of the tracer in liquid and solid	i = L, S
$\bar{\Psi}_{L,G}(s)$	Dimensionless concentration of the tracer in liquid in the Laplace domain	
η	Catalytic effectiveness factor	
ρ_L	Density of the liquid phase	kg m^{-3}
μ_L	Viscosity of the liquid phase	kg m^{-1} s^{-1}

REFERENCES

Al-Dahhan, M. H., Larachi, F., Dudukovic, M. P. and Laurent, A., High-pressure trickle bed reactors: A review. Industrial Engineering Chemical Research, 36, 3292-3314 (1997).

Augier, F., Koudil, A., Muszynski, L. and Yanouri, Q., Numerical approach to predict wetting and catalyst efficiencies inside trickle bed reactors**.** Chemical Engineering Science, v. 65, p. 255-260 (2010).

Ayude, A., Cechini, J., Cassanello, M., Martínez, O. and Haure, P., Trickle bed reactors: Effect of liquid flow modulation on catalytic activity. Chemical Engineering Science, 63, 4969-4973 (2008).

Box, P., A new method of constrained optimization and a comparison with other method. Computer Journal, 8, 42-52 (1965).

Burghardt, A., Grazyna, B., Miczylaw, J. and Kolodziej, A., Hydrodynamics and mass transfer in a three-phase fixed bed reactor with concurrent gas-liquid downflow. Chemical Engineering Journal, 28, 83-99 (1995).

Burghardt, A., Kolodziej, A. S., Jaroszynski, M., Experimental studies of liquid-solid wetting efficiency in trickle-bed cocurrent reactors. Chemical Engineering Journal, 28, 35-49 (1990).

Charpentier, J. C., Favier, M., Some liquid holdup experimental data in trickle bed reactors for foaming and non foaming hydrocarbons, AIChE Journal, 21, 1213-1221 (1975).

Colombo, A. J., Baldi, G. and Sicardi, S., Solid-liquid contacting effectiveness in trickle-bed reactors. Chemical Engineering Science, 31, 1101-1108 (1976).

Dudukovic, M. P., Larachi, F., Mills, P. L., Multiphase reactors-revisited. Chemical Engineering Science, 54, 1975-1995 (1999).

Iliuta, I, Bildea, S. C., Iliuta, M. C. and Larachi, F., Analysis of Trickle bed and packed bubble column bioreactors for combined carbon oxidation and nitrification. Brazilian Journal of Chemical Engineering, 19, 69-87 (2002).

Lange, R., Gutsche, R. and Hanika, J., Forced periodic operation of a trickle-bed reactor. Chemical Engineering Science, 54, 2569-2573 (1999).

Latifi, M. A., Naderifar, A. and Midoux, N., Experimental investigation of the liquid-solid mass transfer at the wall of trickle bed-influence of Schmidt number. Chemical Engineering Science, 52, 4005- 4011 (1997).

Liu, G., Zhang, X., Wang, L., Zhang, S. and Mi, Z., Unsteady-state operation of trickle-bed reactor for dicyclopentadiene hydrogenation. Chemical Engineering Science, 36, 4991-5001 (2008).

Rodrigo, J. G., Rosa, L. and Quinta-Ferreira, M., Turbulence modelling of multiphase flow in high-pressure trickle reactor. Chemical Engineering Science, 64, 1806-1819 (2009).

Ramachandran, P. A. and Chaudhari, R. B., Three Phase Catalytic Reactors. Gordan and Breach, New York, USA, Chap. 7. (1983).

Silva, J. D., Lima, F. R. A., Abreu, C. A. M., Knoechelmann, A., Experimental analysis and dynamic modeling of the mass transfer processes for a fixed bed three-phase reactor in trickle bed regime. Brazilian Journal of Chemical Engineering, 20, n. 4, 375-390 (2003).

Specchia, V., Baldi, G., Pressure drop and liquid holdup for two phase cocurrent flow in packed beds. Chemical Engineering Science, 32, 515-523 (1977).

Tsamatsoulis, D. and Papayannakos, N., Simulation of non ideal flow in a trickle-bed hydrotreater by the cross-flow model. Chemical Engineering Science, 50, 3685-3691 (1995).